Fabrication of suspended dielectric mirror structures via xenon difluoride etching of an amorphous germanium sacrificial layer

Garrett D. Cole,[a] Elaine Behymer, Lynford L. Goddard,[b] and Tiziana C. Bond
Center for Micro- and Nanotechnologies, Lawrence Livermore National Laboratory, Livermore, California 94550

(Received 20 December 2007; accepted 11 February 2008; published 28 March 2008)

The authors present a simplified fabrication method for the creation of free-standing dielectric mirrors for use in monolithic wavelength tunable surface-normal photonic devices, including vertical-cavity surface emitting lasers. This process utilizes a nonplasma dry etching process, based on the noble gas halide, xenon difluoride (XeF_2), to remove an inorganic sacrificial film comprised of low-temperature deposited amorphous germanium (α-Ge). By utilizing nonplasma dry etching of an inorganic film, this procedure circumvents the need for critical point drying and avoids the limitations imposed by polymer-based sacrificial layers. In this procedure the authors observe remarkably rapid lateral etching, with rates in excess of 150 μm/min for electron-beam evaporated α-Ge films. The viability of this novel surface micromachining process is demonstrated by presenting the static and dynamic mechanical characteristics of electrostatically actuated suspended dielectric Bragg reflectors. © *2008 American Vacuum Society.* [DOI: 10.1116/1.2890673]

I. INTRODUCTION

Due to their compact nature and potential for low cost wafer-scale fabrication techniques, micromechanically tunable surface-normal photonic devices including vertical-cavity surface-emitting lasers (VCSELs),[1–3] amplifiers,[4,5] modulators,[6] and filters[7] have attracted interest for use in a variety of applications ranging from communications[8] to spectroscopy.[9] In these devices, the vertical orientation of the cavity, which results in optical resonance perpendicular to the wafer surface, allows for facile integration of microelectromechanical systems (MEMS). In MEMS-tunable vertical-cavity devices, wavelength tuning is achieved by displacing a suspended mirror relative to a fixed reflector in order to alter the resonance condition of the Fabry-Pérot cavity, with electrostatic or electrothermal actuators being the most commonly implemented. As compared to more complex multisection in-plane devices,[10] with micromechanical structures, wavelength tuning can be realized through the control of a single tuning voltage (or current). Additionally, as a result of the short axial cavity length in vertical-cavity resonators, it is possible to achieve continuous mode-hop-free tuning over a wide wavelength range through direct variation of the optical path length.

Because MEMS-tunable structures rely on physical path length changes, an air gap must be incorporated within the optical cavity. While such a configuration is advantageous in that it provides a relatively simple means to achieve wavelength tuning, in practice, the fabrication procedures used to realize the suspended mirror have been relatively complex, requiring the assembly of two disparate chips,[1,11] polymer processing for definition of the sacrificial layer,[2,6] and CO_2 critical point or sublimation drying in the case of wet-etched sacrificial layers.[3–7] Specifically for monolithic structures, the most common means of generating the suspended mirror has been through the selective removal of a sacrificial film (both organic and inorganic) using a suitable wet chemical etchant[3–7] or via oxygen-plasma based dry etching for polymer sacrificial layers.[2] With wet chemistry mediated undercutting, critical point drying or solvent sublimation is required to avoid the collapse of the suspended mirror structure due to surface tension forces in the evaporating liquid. In the case of organic sacrificial layers, devices that rely upon the polymer as a permanent portion of the materials stack have the potential for degraded reliability due to environmental effects. Additionally, the incorporation of polymer layers places severe constraints on the maximum processing temperature of the structural films and dielectric mirror stack, limited by the glass-transition temperature or thermal decomposition of the material. This limitation in thermal budget excludes the use of high temperature or high plasma-energy processes for the deposition of high quality films for the suspended DBR. Finally, the incorporation of organic films as the sacrificial layer (both permanent and temporary) limits the chemistry that the sample may be exposed to in the course of, or following, fabrication.

In this work we present a novel surface micromachining procedure for the production of suspended dielectric distributed Bragg reflectors (DBRs) that overcomes the aforementioned limitations. This process makes use of the noble gas halide, xenon difluoride (XeF_2), to rapidly undercut an amorphous germanium (α-Ge) sacrificial layer. Such a method enables nonplasma, dry selective etching of an inorganic sacrificial film, alleviating the need for critical point drying and resulting in sacrificial layer removal with nearly infinite selectivity over most metals, dielectrics, III-V compounds, etc. Furthermore, the use of α-Ge for the sacrificial film allows for more flexibility in processing compared to structures utilizing polymer sacrificial layers. With α-Ge sacrificial layers,

[a]Electronic mail: cole35@llnl.gov
[b]Present address: Micro and Nanotechnology Laboratory, University of Illinois at Urbana-Champaign, Urbana, IL 61801.

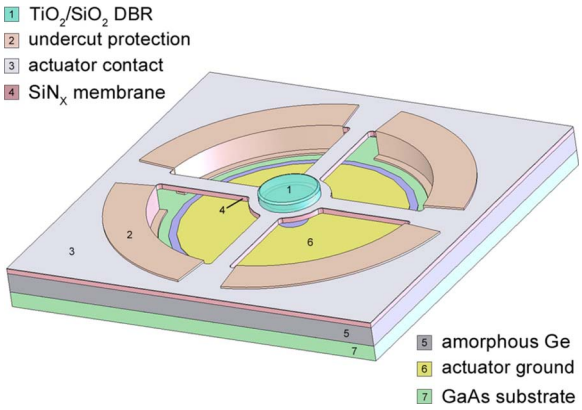

FIG. 1. Solid model of the suspended mirror structure. The numbers (colors) indicated in the legend denote the various layers making up the device, starting from the top down.

the fabrication procedure may be tailored to utilize low temperature steps (<200 °C), allowing for the realization of suspended DBRs on nearly any relevant substrate. On the other hand, the chemical stability of germanium thin films can provide a solid foundation for elevated temperature deposition processes that are not compatible with polymer sacrificial layers, which may be desired for high-quality structural or optical films.

II. DESIGN AND FABRICATION

Figure 1 presents a solid model of the suspended mirror structure presented in this manuscript. This device utilizes a mechanical design identical to wavelength tunable vertical-cavity semiconductor optical amplifiers demonstrated previously.[4,5] In contrast to the epitaxial devices developed in that research effort, which utilized a suspended AlGaAs-based DBR, the tunable mirror design discussed here incorporates a silicon nitride (SiN_x) membrane capped by an evaporated dielectric DBR. The use of the dielectric suspended mirror structure allows for the development of a platform-independent tuning mechanism that may be integrated with various materials systems including GaAs, InP, GaSb, GaN, and related alloys. The flexibility in operating wavelength afforded by the dielectric MEMS structure is useful for applications such as optical gas sensing where key absorption lines may span a region larger than that attainable by a single materials system.

From the top down, the suspended mirror consists of a seven-period TiO_2/SiO_2 dielectric DBR on top of a SiN_x structural film. The combination of the TiO_2/SiO_2 stack and nitride membrane forms a suspended reflector, including the SiN_x film as a high index quarter-wave layer. In this mirror structure, the large index discontinuity between the membrane and air gap leads to a significant enhancement in the reflectivity for a given number of mirror periods. To achieve displacement of the suspended DBR, and thus tuning of the cavity resonance wavelength, the device incorporates an integrated electrostatic actuator. In this implementation an applied bias across the aluminum layer on top of the SiN_x structural film and the gold ground pad generates a Coulomb force that deflects the DBR toward the substrate. When combined with a suitably designed optical cavity,[5] this deflection results in a reduction of the optical path length and a blueshift in the resonance wavelength. As discussed previously, the large free-spectral range of vertical microcavities allows for wide and continuous resonance tuning. For the devices presented here, the use of the integrated electrostatic actuator allows for a rapid tuning response. Previous characterization of microactuators using an identical mechanical layout has demonstrated a near-critically damped temporal response at atmospheric pressure with a sub-10-μs switching speed.[12]

Fabrication of the suspended mirror structure begins with the definition of the lower electrode for the electrostatic actuator. In this case the device utilizes an evaporated Ti/Au contact pad (with a small central aperture to allow optical transmission) defined by liftoff on an *n*-doped GaAs substrate. Following the bottom contact definition, a germanium sacrificial layer is deposited via electron-beam evaporation. This process is carried out at a base pressure below 1×10^{-6} Torr with the samples clipped to a rotating substrate holder for improved thickness uniformity. In this system the sample holder also incorporates a resistive heating element; thus, we have investigated various deposition temperatures ranging from room temperature to 200 °C. Under these conditions the deposited films show no change in surface morphology or etch rate, and, as a result, the samples presented in this manuscript have utilized room temperature germanium deposition. It is important to note that evaporation is carried out with the germanium source material placed in direct contact with the copper hearth, without the use of a ceramic crucible, as early tests showed spitting of the germanium source when the material was placed in a liner. Under these conditions we can routinely produce smooth α-Ge films with surface roughness values approaching that of the substrate for deposition rates up to 4 Å/s. Previous investigations of the structural properties of evaporated α-Ge thin films have reported root-mean-square roughness values ranging from 8 to 11 Å.[13,14] Note that an excellent surface quality is required for the sacrificial layer in these devices, as any excess roughness will be transferred to the dielectric mirror stack, resulting in reduced reflectivity and increased scattering loss in the optical cavity.

Following the α-Ge evaporation process, a SiN_x structural film is deposited via plasma-enhanced chemical-vapor deposition (PECVD) using a dilute silane mixture at 200 °C, producing an intrinsic tensile stress of 328 MPa. Because this film serves as the first high index layer in the suspended DBR, the thickness is constrained to be an odd-multiple of $\lambda/4$. Next, an aluminum film (1500 Å) is evaporated. This layer serves as the top electrode of the electrostatic actuator. After deposition, a window is opened in the aluminum by wet chemical etching, allowing for optical transmission through the opaque contact layer as with the lower Ti/Au electrode. A blanket electron-beam evaporation of seven pe-

riods of alternating quarter-wave TiO_2/SiO_2 forms the remainder of the dielectric reflector and completes the materials structure of the suspended mirror.

Following the mirror deposition process, the DBR pillar is defined by electron cyclotron resonance etching of the TiO_2/SiO_2 stack with a SF_6/Ar chemistry analogous to that described in Ref. 15. In this process the aluminum top contact serves as an etch stop and displays excellent selectivity,[16] thus alleviating the need for a precisely timed etch or end-point monitoring through optical or spectroscopic means. Subsequent to the DBR pillar definition, the actuator geometry is defined by wet chemical etching through the aluminum film, and then dry etching through the SiN_x membrane and α-Ge sacrificial layer with a CF_4/O_2 plasma. In this case the gold contact pad and GaAs substrate serve as an etch stop for the actuator definition. Next, a SiO_2 film is patterned by liftoff, following a low-temperature (100 °C) PECVD process. This feature serves to reduce excessive underetching of the sacrificial layer beneath the supports and improves the control over the initial position of the suspended mirror.[5,17]

To create the air gap, the sacrificial α-Ge layer is selectively dry etched by exposing the sample to XeF_2 at an etch pressure of 1 Torr. For this procedure we employ a pulsed XeF_2 etching system based on the tool described in Ref. 18—note that this reference discusses the details of the mechanical design of the etcher as well as the proposed etch mechanism and selectivities (in this case for reactions involving silicon, although it is assumed to be analogous for germanium). Although this process has been applied extensively in silicon-based microfabrication, to the best of our knowledge, this is the first use of XeF_2 for the development of micromechanical devices on a compound semiconductor substrate.

When compared with other candidate micromachining techniques, the XeF_2 etching process exhibits a number of advantages. On one hand, it allows for real-time observation of the release etch, affording the ability to monitor the progression of the lateral etch front *in situ*—note that the ability to view the lateral etch length in real time is exceedingly difficult, if not impossible, in the case of plasma or wet chemical etching. As a second benefit, the XeF_2 procedure not only alleviates the need for critical point drying, but also allows the process to be repeated if the etch has not fully terminated. This is in contrast to wet-chemistry-based undercut etching, where surface tension forces may block fluids from penetrating into the micrometer scale gaps beneath partially etched membranes.

III. RESULTS AND DISCUSSION

This process has enabled the fabrication of on-chip two-dimensional arrays of tunable mirror structures suitable for devices such as MEMS-tunable VCSELs. Figure 2(a) displays an optical micrograph of a 4.4×4.4 mm^2 area of the wafer postprocessing, demonstrating the ability to define two-dimensional arrays of monolithically integrated suspended mirror structures. In part (b) of the same figure, a close-up view of a single device is included. In the current lithographic layout each device is surrounded by a thick aluminum bond-pad as well as trenches (penetrating through the α-Ge layer) for achieving electrical isolation between neighboring actuators. From the figure it is apparent that this process allows for excellent actuator yield. Postprocess destructive characterization has demonstrated outstanding adhesion of the deposited films to the underlying GaAs substrate.

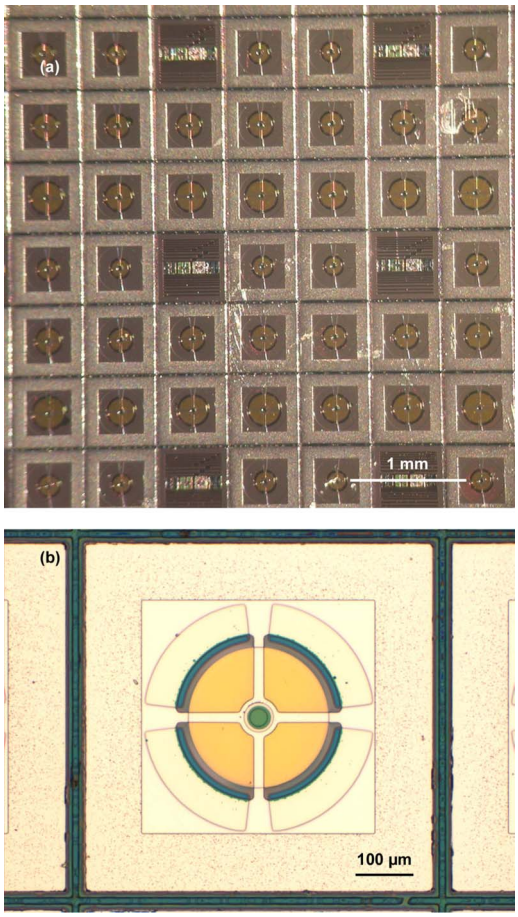

FIG. 2. (a) Two-dimensional array of suspended DBR structures. Note the inclusion of fixed-fixed and cantilever beam structures for film stress characterization. (b) Close-up view of a single actuator surrounded by an aluminum bond pad and electrical isolation trenches.

Line scans of the suspended mirror structure generated with a white-light profilometer reveal a slight out-of-plane bowing of the membrane following release, as depicted in Fig. 3, with typical initial deflection values of +150 nm (resulting in an air-gap thickness of ~1150 nm). Fortunately, all devices display bowing away from the substrate, which may easily be overcome through additional actuation. The initial deflection is most likely driven by uncompensated strain in the TiO_2/SiO_2 DBR stack.

One interesting aspect of this fabrication method is the particularly rapid nature of the underetching process. For a XeF_2 etch pressure of 1 Torr, the evaporated α-Ge films exhibit lateral etch rates greater than 150 μm/min. In fact, for the devices presented in this manuscript, the total time required to successfully undercut an 80 μm diameter mem-

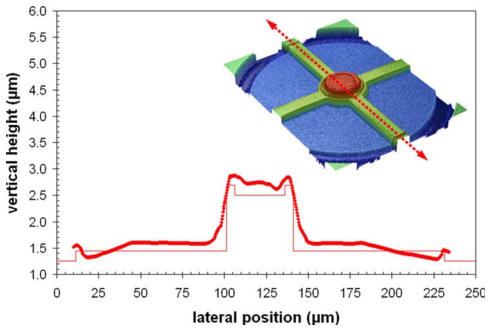

FIG. 3. Line scan of the suspended mirror recorded with an optical profilometer; the inset includes the original three-dimensional mapping and indicates the path of the two-dimensional plot. The ideal profile, utilizing nominal thickness values, is depicted along with the measured data points. A minor upward bowing is revealed, leading to an initial vertical position of ~1600 nm compared with the nominal value of 1450 nm (measured from the surface of the aluminum contact to the gold ground plane). This bowing extends the nominal 1000 nm air gap to 1150 nm.

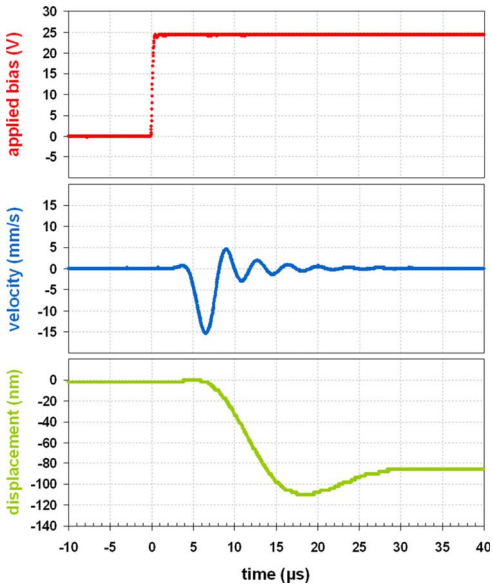

FIG. 4. Step response of the suspended mirror at atmospheric pressure for a bias of 24 V; negative values indicate vertical motion toward the substrate. Ringing in this structure leads to a settling time of just under 30 μs. Note that the vibrometer has a 3 dB bandwidth of 250 kHz for velocity and 50 kHz for displacement measurements.

brane was less than 20 s (achieved through two 10 s pulses or one single 20 s etch pulse). These etch rates far exceed those recently demonstrated for crystalline germanium, which approached 50 μm/min at a XeF_2 pressure of 0.8 Torr,[19] as well as the maximum reported silicon rate of ~10 μm/min at 2.6 Torr.[16] Beyond simple geometrical effects, we hypothesize that the decreased density of the evaporated films leads to an enhancement in the etch rate. Further investigation will be necessary to elucidate the underlying mechanism of this extreme reaction rate.

Although the discussion has, thus far, focused solely on evaporated α-Ge-based sacrificial layers, it is important to note that the same basic procedure may be extended to structures incorporating poly- or single-crystalline Ge, Si, or Si_xGe_{1-x} alloys as the sacrificial material, deposited with a variety of techniques including epitaxy, CVD, sputtering, pulsed laser deposition, etc. As with α-Ge, these materials may be readily etched with XeF_2, while still realizing all of the previously discussed advantages. Furthermore, the suspended mirror structure is not limited to a planar configuration. In these devices half-symmetric cavities may be generated via strain engineering of the DBR stack,[1,2] or through microlens formation[20] on the surface of the germanium (or related alloy) prior to depositing the structural film and mirror layers.

To demonstrate the viability of our suspended mirror structures, we present a characterization of the static and dynamic properties of the actuator using a laser-Doppler-vibrometer-based MEMS motion characterization system similar to that described in Ref. 21. Figure 4 presents the step response characteristics for an actuator with a 60 μm diameter central membrane and 70 μm long by 20 μm wide tethers. It is important to note that the data presented in the figure exhibit temporal smoothing as the 3 dB bandwidth of the vibrometer (250 kHz for velocity and 50 kHz for displacement) results in rise times of approximately 1.4 and 7.0 μs, respectively. In this experiment the bottom gold pad is held at ground and the bias is applied to the top aluminum contact. Actuation is recorded in open air under a long working distance objective to allow for electrical probing of the devices. From the step response data it is clear that ringing is limiting the response time of these structures. Regardless, these results verify the rapid nature of the electrostatic tuning mechanism; for the data displayed below, the actuator reaches equilibrium displacement in approximately 30 μs. In these devices the settling time may be further reduced by optimizing the geometry of the actuator to achieve sufficient squeeze-film damping for a near-critically damped response.[12]

By recording the equilibrium displacement values as a function of the actuation voltage, the quasi-static deflection characteristics of the suspended mirror may be generated from the step response results. The compiled displacement versus bias data for an actuator with a similar geometry to that described above is included in Fig. 5. As shown in the figure, the device under test reaches a deflection of 224 nm for an applied bias of 30 V. In this plot the theoretical curve has been generated through an iterative solution to the analytical electromechanical model presented in Ref. 5. From the theoretical model, the estimated snap-down voltage (displacement) is 30.9 V (447 nm) with the best fit achieved for an air-gap thickness of 1120 nm. This value compares well with the profilometer derived air-gap thickness of ~1150 nm. Assuming this mirror was incorporated on a GaAs-based 1-λ semiconductor cavity with a hypothetical center wavelength of 1000 nm, the measured deflection would result in a wavelength tuning range of 37 nm at 30 V bias (this calculation includes the penetration depth for a 25.5 period GaAs/AlAs bottom DBR).

Devices with longer spring lengths and larger diameter central membranes allow for a reduced maximum tuning

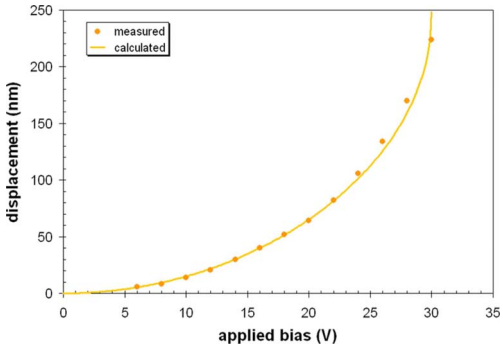

FIG. 5. Theoretical and experimental static deflection characteristics of the suspended mirror structure (geometry described in the text). Experimental displacement values are extracted from step response measurements for square wave drive voltages up to 30 V. The theoretical curve is generated from the iterative solution of the one-dimensional electromechanical model presented in Ref. 5.

voltage; for example, we have characterized structures with a 70 μm diameter central membrane with a spring length of 95 μm that exhibit 292 nm of displacement at an applied bias of 20 V. One of the benefits of the electrostatic actuator is the extremely low power consumption. For the capacitive structure presented here, current-voltage characterization has verified the leakage current to be less than 20 pA at 30 V.

IV. SUMMARY AND CONCLUSIONS

We have demonstrated a novel surface micromachining process for the production of suspended dielectric DBRs for use in MEMS-tunable surface normal photonic devices. This process relies on the noble gas halide, XeF_2, to remove an inorganic sacrificial film comprised of evaporated α-Ge. This procedure alleviates the need for critical point drying, as required in wet-chemical undercutting schemes, and avoids the limitations imposed by the use of polymer sacrificial layers.

Although this manuscript has focused solely on amorphous germanium, it is important to note that poly- or single-crystalline germanium, silicon, or silicon-germanium alloys would be viable alternatives for the sacrificial layer in this process. As an interesting observation, the use of evaporated amorphous germanium films allows for a truly remarkable lateral etch rate, exceeding 150 μm/min for a XeF_2 etch pressure of 1 Torr.

Finally, this procedure has been utilized to demonstrate high performance two-dimensional arrays of freely suspended micromirrors. The completed devices exhibit excellent yield as well as adequate control over the initial position of the suspended mirror. Through the use of an integrated electrostatic actuator, maximum displacement—limited by the instability of the electrostatic actuator—is realized with tuning voltages ranging from 20 to 30 V (dependent on the actuator geometry). Moreover, the devices demonstrate the potential for rapid tuning, with settling times below 30 μs. Thus, this procedure has been proven to be successful for the development of tunable mirror structures that may be incorporated in micromechanically tunable surface normal photonic devices such as tunable VCSELs, amplifiers, detectors, filters, etc.

ACKNOWLEDGMENTS

This work was performed under the auspices of the U.S. Department of Energy by Lawrence Livermore National Laboratory under Contract No. DE-AC52-07NA27344.

[1]M. Maute, B. Kögel, G. Bohm, P. Meissner, and M.-C. Amann, IEEE Photon. Technol. Lett. **18**, 688 (2006).
[2]Y. Matsui, D. Vakhshoori, P. Wang, P. Chen, C.-C. Lu, M. Jiang, K. Knopp, S. Burroughs, and P. Tayebati, IEEE J. Quantum Electron. **39**, 1037 (2003).
[3]M. C. Y. Huang, K. B. Cheng, Y. Zhou, A. P. Pisano, and C. J. Chang-Hasnain, IEEE J. Sel. Top. Quantum Electron. **13**, 374 (2007).
[4]G. D. Cole, E. S. Björlin, C. S. Wang, N. C. MacDonald, and J. E. Bowers, IEEE Photon. Technol. Lett. **17**, 2526 (2005).
[5]G. D. Cole, E. S. Björlin, Q. Chen, C.-Y. Chan, S. Wu, C. S. Wang, N. C. MacDonald, and J. E. Bowers, IEEE J. Quantum Electron. **41**, 390 (2005).
[6]W. S. Rabinovich, T. H. Stievater, N. A. Papanicolaou, D. S. Katzer, and P. G. Goetz, Appl. Phys. Lett. **83**, 1923 (2003).
[7]A. Hasse, S. Irmer, J. Daleiden, N. Dharmarasu, S. Hansmann, and H. Hillmer, Electron. Lett. **42**, 974 (2006).
[8]J. S. Harris, IEEE J. Sel. Top. Quantum Electron. **6**, 1145 (2000).
[9]B. Kögel, H. Halbritter, S. Jatta, M. Maute, G. Böhm, M.-C. Amann, M. Lackner, M. Schwarzott, F. Winter, and P. Meissner, IEEE Sens. J. **7**, 1483 (2007).
[10]L. A. Coldren, G. A. Fish, Y. Akulova, J. S. Barton, L. Johansson, and C. W. Coldren, J. Lightwave Technol. **22**, 193 (2004).
[11]N. Kanbara, S.-i. Tezuka, and T. Watanabe, in Proceedings of IEEE/LEOS International Conference on Optical MEMS and Their Applications (MOEMS 2006), Big Sky, MT, 21–24 August 2006, paper no. MA3.
[12]G. D. Cole, J. E. Bowers, K. L. Turner, and N. C. MacDonald, in Proceedings of IEEE/LEOS International Conference on Optical MEMS and Their Applications (MOEMS 2005), Oulu, Finland, 1–4 August 2005, paper no. F4.
[13]H. Rafla-Yuan, J. D. Rancourt, and M. J. Cumbo, Appl. Opt. **36**, 6360 (1997).
[14]G. Pérez, A. M. Bernal-Oliva, E. Márquez, J. M. González-Leal, C. Morant, I. Génova, J. F. Trigo, and J. M. Sanz, Thin Solid Films **485**, 274 (2005).
[15]G. Dang, H. Cho, K. P. Ip, S. J. Pearton, S. N. G. Chu, J. Lopata, W. S. Hobson, L. M. F. Chirovsky, and F. Rena, J. Electrochem. Soc. **148**, G25 (2001).
[16]K. R. Williams and R. S. Muller, J. Microelectromech. Syst. **5**, 256 (1996).
[17]S. Irmer, J. Daleiden, V. Rangelov, C. Prott, F. Romer, M. Strassner, A. Tarraf, and H. Hillmer, IEEE Photon. Technol. Lett. **15**, 434 (2003).
[18]P. B. Chu, J. T. Chen, R. Yeh, G. Lin, J. C. P. Huang, B. A. Warneke, and S. J. Pister, 9th International Conference on Solid State Sensors and Actuators, Digest of Technical Papers Transducers '97, Chicago, IL, 16–19 June 1997, paper no. 2D3.01, p. 665.
[19]G. Xuan, T. N. Adam, J. Suehle, E. Fitzgerald, P. Lv, N. Sustersic, M. J. Coppinger, and J. Kolodzey, in Proceedings of the Third International SiGe Technology and Device Meeting (ISTDM 2006), Princeton, NJ, 15–17 May 2006, paper no. 5P.44.
[20]E. M. Strzelecka, G. D. Robinson, L. A. Coldren, and E. L. Hu, Microelectron. Eng. **35**, 385 (1997).
[21]K. L. Turner, P. G. Hartwell, and N. C. Macdonald, 10th International Conference on Solid State Sensors and Actuators, Digest of Technical Papers Transducers '99, Sendai, Japan, 7–10 June 1999 (unpublished), p. 1144.